Applied Physics Express

The Japan Society of Applied Physics

LETTER

Enhancing the light extraction of AlGaN-based vertical type deep-ultraviolet light-emitting-diodes with an internal reflector

To cite this article: Youn Joon Sung *et al* 2019 *Appl. Phys. Express* **12** 122011

Applied Physics Express 12, 122011 (2019)
https://doi.org/10.7567/1882-0786/ab52b6

LETTER

Enhancing the light extraction of AlGaN-based vertical type deep-ultraviolet light-emitting-diodes with an internal reflector

Youn Joon Sung[1,2], Young-Gyeong Lee[1], Hwankyo Kim[1], Hyun-Soo Lim[1], O-Min Kwon[1], Sunghan Choi[1], Yong-Tae Moon[1], Rak-Jun Choi[1], Myung-Hoon Jung[1], Jeong-Tak Oh[1], Dong Woo Kim[2], and Geun Young Yeom[2,3*]

[1]Department of LED Business, Chip development group, LG Innotek, Paju, 10842, Republic of Korea
[2]School of Advanced Materials Science and Engineering, Sungkyunkwan University, Suwon 16419, Republic of Korea
[3]SKKU Advanced Institute of Nano Technology (SAINT), Sungkyunkwan University, Suwon 16419, Republic of Korea

*E-mail: gyyeom@skku.edu

Received September 11, 2019; revised October 11, 2019; accepted October 30, 2019; published online November 13, 2019

AlGaN-based UV-C vertical LEDs comprising Ga-face *n*-contact and an internal reflector are reported here. Inside the chip, the internal reflector is designed as a hexagonal shape surrounding a circular *n*-electrode. The use of SiO_2/Al reflectors on the etched plane improves the local reflectivity. Forming the internal reflector has been shown to lead to a significant improvement in light output power (LOP). The LOP of the vertical LED with an internal reflector is 1.27 times higher than that of the vertical LED without an internal reflector.

Aluminum gallium nitride (AlGaN)-based deep-ultraviolet lighting emitting diodes (DUV LEDs) have attracted attention for use in a variety of potential applications including water purification, surface disinfection, biomedicine, detection of material, phototherapy, and UV curing.[1–4] However, due to the low external quantum efficiencies and the low LOP, which are mainly attributable to their poor light extraction efficiency (LEE),[5–9] DUV LEDs have proven difficult to commercialize. In particular, regarding AlGaN-based LEDs, the transverse magnetic (TM)-polarized light, which becomes dominant as the emission wavelength decreases, mainly propagates parallel to the *c*-plane sapphire. Therefore, TM-polarized light emitted from the multi quantum well (MQW) has to travel a long distance before light extraction and eventually suffers from poor light extraction due to the large optical loss.[10–12] The LEE is also affected by the absorptive GaN layer,[13] the current crowding due to highly resistive AlGaN[14,15], and the inclined angle of the mesa sidewall by strongly affecting the propagation of the TM-polarized light. Recent studies have attempted to improve the LOP by applying a reflector to the mesa sidewalls of conventional chip structures in DUV LEDs. Chen et al.[16] reported that for mesa structures, an inclination angle of 37.83° was the optimal angle to improve LEE, and that a SiO_2/Al mirror inclined mesa sidewall further enhanced the LEE Lee et al.[17] showed that a multi mesa stripes structure with a MgF_2/Al mirror on the inclined sidewall achieved improved LEE. Even though the *p*-AlGaN is transparent in the DUV region, it is difficult to increase the conductivity of *p*-AlGaN with increasing Al composition due to the relatively high work function that is not favorable for ohmic contact, even with high Mg doping.[18,19] Therefore, *p*-GaN, which strongly absorbs UV light, is typically used as a *p*-contact layer in DUV LEDs,[20–22] and the selective removal of *p*-GaN and the formation of a reflective electrode on the exposed *p*-AlGaN are used to minimize the absorption and to enhance the reflectivity.[23,24]

DUV LEDs generate a lot of heat due to their low efficiency, and they also need to be driven at high current to obtain high LOP.[25] Therefore, a device structure with efficient heat dissipation and low series resistance is necessary. The vertical LED is one of the promising candidates in DUV LEDs due to its high thermal conductivity and the short path between *n*- and *p*-electrodes.[26–28] The main emission occurs at the edge of the mesa due to the current crowding effect. In order to increase the emission area, the total circumference length of the mesa edge needs to be increased. Hao et al.[29] and Zhang et al.[30] reported that increasing the *p*-electrode perimeter and optimizing the *p*-electrode design in consideration of the current spreading length increased the effective emission area. The longer perimeter leads to decreased total resistance, which results in reductions in Joule heating and junction temperature. The vertical LED with the Ga-face *n*-contact has a longer circumference length along with easier *n*-contact formation than conventional vertical LEDs with the N-face *n*-contact.

In this paper, we report on the Ga-face *n*-contact type vertical LED with an internal reflector. In order to improve the LOP, an internal reflector is applied around the circular *n*-electrodes of the vertical LED. By reflecting the TM-polarized light, the LOP can be increased. With the application of an internal reflector, a significant improvement of LOP with 280 nm UV-C LEDs has been demonstrated.

Here, the AlGaN-based UV-C LED structure has been grown on a sapphire substrate. The UV-C LED structure includes a 3.0 μm thick AlN, a 200 nm thick AlGaN for laser lift-off (LLO) formation, a 3.0 μm thick Si-doped *n*-AlGaN, five pairs of AlGaN/AlGaN MQWs, a 35 nm thick Mg-doped *p*-AlGaN electron blocking layer, and a 450 nm thick Mg-doped *p*-GaN for *p*-ohmic contact. After the UV-C LED structure has been grown, two types of vertical chips are fabricated in order to investigate the effects of an internal reflector on the LOP. The chip size is $1 \times 1\ mm^2$. One of these types is a vertical LED with an internal reflector while the other type does not have an internal reflector. The Ti/Al/Ni/Au is used for the *n*-electrode and the Ni/Au layer is used for the *p*-ohmic contact. To form a vertical LED with an internal reflector, honeycomb-shaped trenches are formed around the *n*-electrodes through reactive ion etching, followed by the deposition of SiO_2 and Al. The subsequent processes are the same as those used for the vertical LEDs without an internal reflector. First, the *n*-type and *p*-type electrodes are spatially separated by an insulator to prevent electrical connections. Then, bonding metals are deposited to combine the LED wafer with a carrier wafer by thermal compression at a temperature of 300 °C. Next, the LLO process is carried out using a high energy laser to separate and transfer the LED structure from the sapphire to the carrier

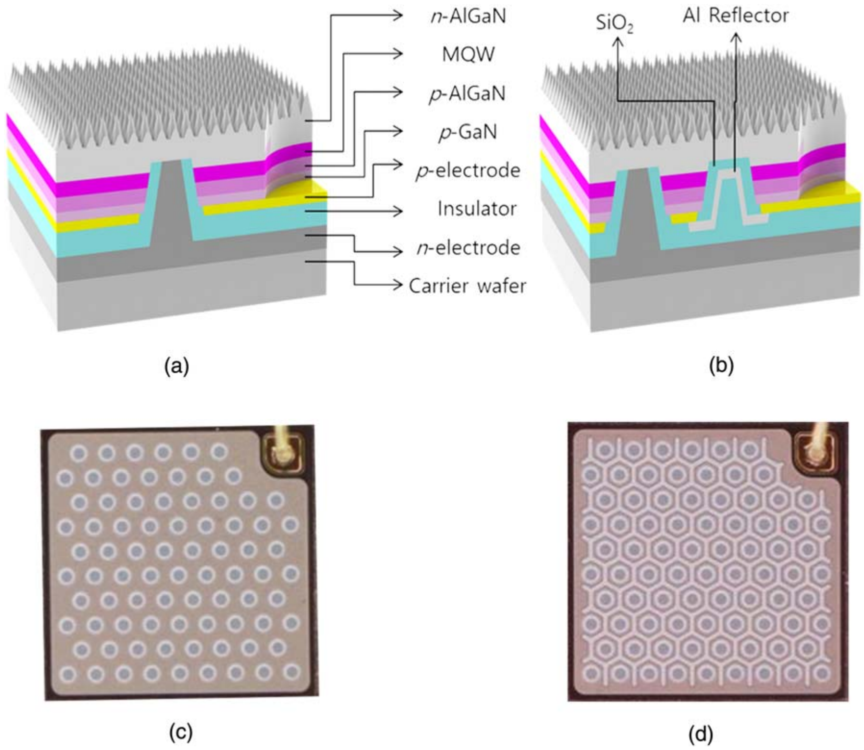

Fig. 1. (Color online) Schematic drawings of AlGaN-based UV-C vertical LEDs (a) without and (b) with an internal reflector. Optical microscopic images of the 1×1 mm^2 vertical LEDs (c) without and (d) with an internal reflector.

wafer. Following the LLO process, the sapphire substrate is removed. The UV-C LED structure on the carrier wafer is dipped into a HCl solution to remove Al and Ga droplets. Next, the *n*-AlGaN is roughened by an alkali solution, and each chip is isolated by dry etching. The chips, which are not encapsulated by resin or lenses, are attached to the 6060 PKG. The LOP of the vertical LED is measured using an integrating sphere.

Figures 1(a) and 1(b) show schematic drawings of the vertical LEDs without and with an internal reflector, respectively. Optical microscopic images of vertical LEDs made without and with an internal reflector are also shown in Figs. 1(c) and 1(d). The circular shapes in the chip are the *n*-electrode image shown in Figs. 1(c) and 1(d), while the honeycomb-shaped hexagonal lines surrounding the *n*-electrodes in Fig. 1(d) are the internal reflectors.

Figure 2 shows a cross-sectional SEM image of the internal reflector in the vertical LED with an internal reflector. The trench sidewall has an inclination of 30° with SiO_2/Al stacked sequentially. The inclination of the trench sidewall is formed so that the reflected light can propagate to the upper direction and eventually be extracted to the outside of the device through the roughened surface. In addition, the position of the internal reflector is formed by etching 500 nm deeper than the MQWs in order to sufficiently reflect the TM-polarized light.

Figure 3 shows the (a) LOP–current–voltage (L–I–V) and (b) current–external quantum efficiency (I–EQE) characteristics of the UV-C vertical LEDs with/without an internal reflector. As shown in Fig. 3(a), the LOPs are 14.3 mW for the vertical LED without an internal reflector and 18.2 mW for the vertical LED with an internal reflector at an injection current of 200 mA with a peak wavelength of about 280 nm. The voltages of the vertical LED without and with an internal

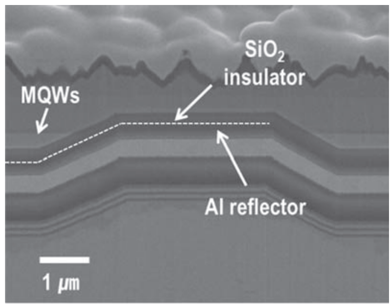

Fig. 2. Cross-sectional SEM image of the internal reflector region. Internal reflector comprises SiO_2 and highly reflective Al.

reflector were 5.94 V and 5.89 V at the same current, respectively. The voltage differences between the two structures are negligible because the current is concentrated mainly at the mesa edge area by the current crowding effect not at the internal reflector area which is located far from the mesa hole. The vertical LED with an internal reflector has a LOP that is 27% higher than that of the vertical LED without an internal reflector. The improvement in the LOP of the vertical LED with an internal reflector indicates an increase in the number of photons extracted by reflecting TM-polarized light. In the propagation of light to the surface direction, the light propagating with an incident angle greater than the escape angle is re-entered to the LED direction due to the total internal reflection effect. The re-entry light can be further extracted by reflecting on the etched plane of the internal reflector. The vertical LED with an internal reflector increases the LOP due to an improvement in the reflectivity. Figure 3(b) shows that the EQE of the vertical LED without and with an internal reflector are 1.60% and 2.07% at an injection current of 200 mA, respectively. These results show that the vertical LED with an internal reflector improves the

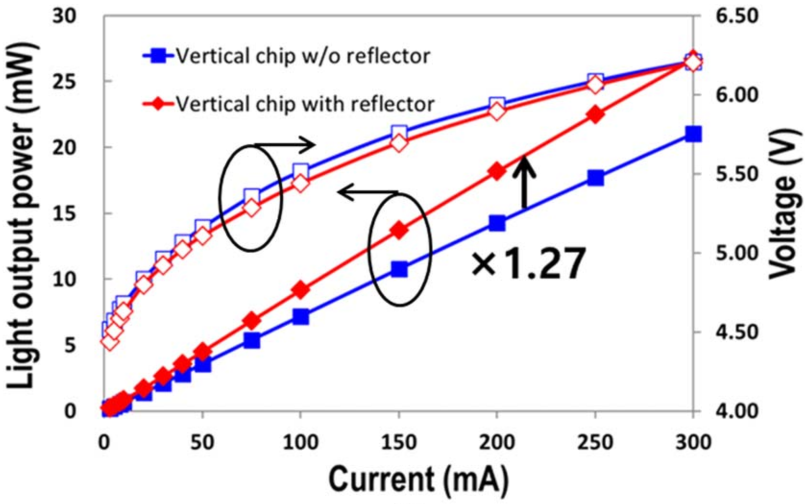

(a)

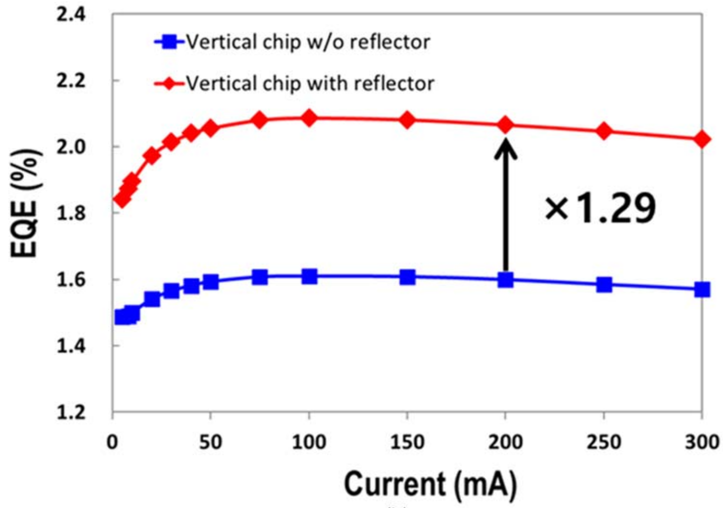

(b)

Fig. 3. (Color online) (a) Light output power–current–voltage (*L–I–V*) and (b) *I*–EQE characteristics of UV-C vertical LEDs without and with an internal reflector.

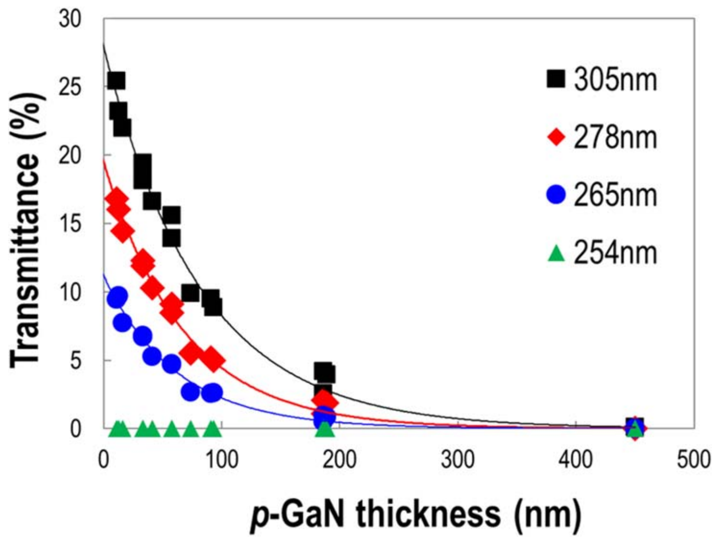

Fig. 4. (Color online) Transmittance of UV-C LED (light) on sapphire as a function of *p*-GaN layer thickness. Each solid is the measured transmittance of different wavelength for different *p*-GaN thickness. Each solid line indicates the fitting line for different wavelength obtained from Eq. (1).

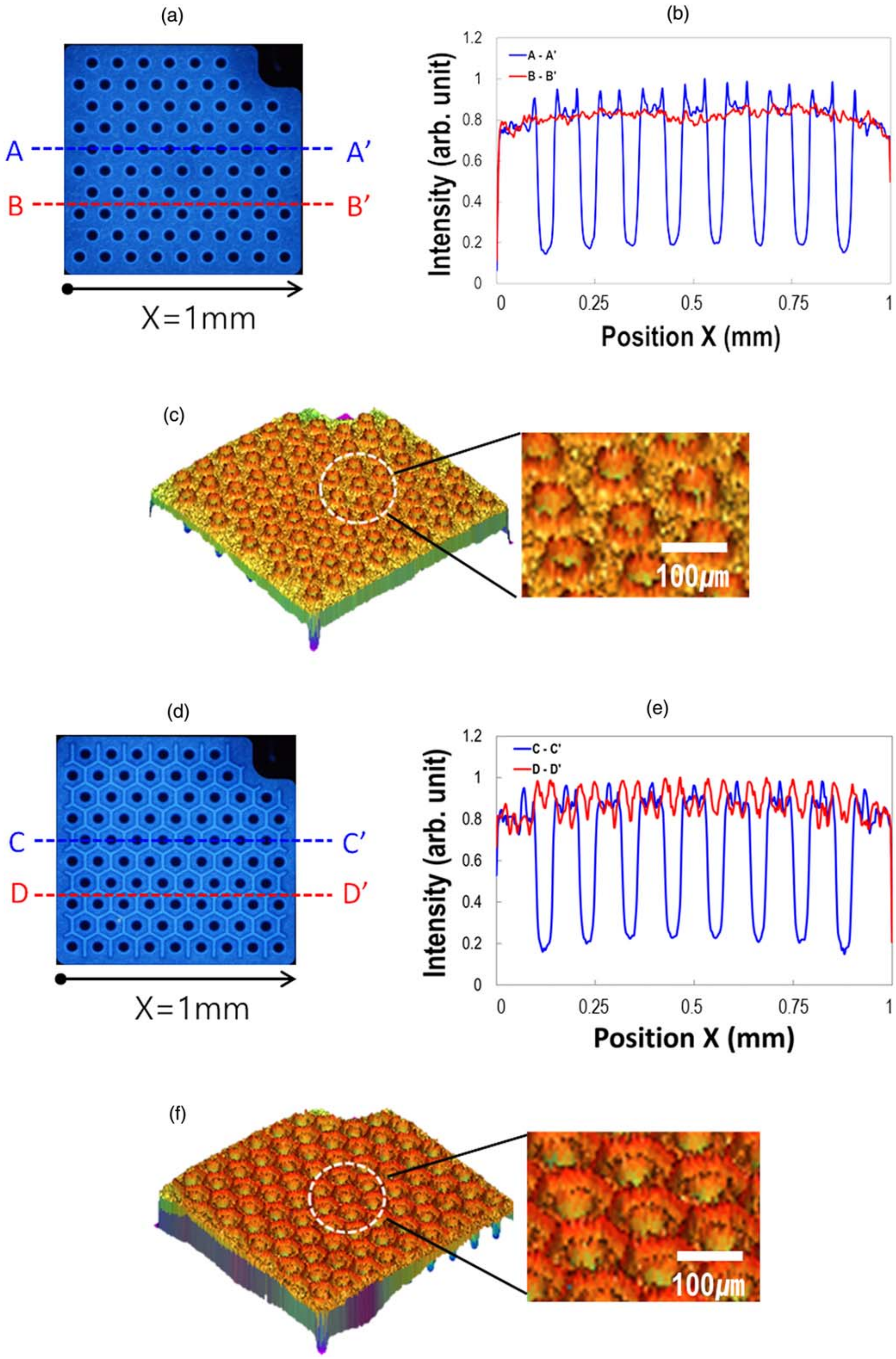

Fig. 5. (Color online) (a) CCD image of light emission, (b) line-profile of emission distribution, and (c) three-dimensional emission distribution of vertical LED without an internal reflector at an injection current of 200 mA. (d) CCD image of light emission, (d) line-profile of light emission distribution, and (f) three-dimensional light emission distribution of vertical LED with an internal reflector at an injection current of 200 mA.

EQE compared to the vertical LED without an internal reflector, which is attributed to the increased LEE.

Although the light propagation to the surface direction is extracted as mentioned above, most of the light propagating to the direction of the *p*-GaN is absorbed. Because the removal of the *p*-GaN may partly increase the LOP by reducing the absorption effect, the effect of *p*-GaN thickness on transmittance and absorption may need to be investigated. Figure 4 shows the transmittance of UV-C LED (light) as a function of the remaining *p*-GaN thickness. The transmittance is measured until the 450 nm thick *p*-GaN is removed by etching the *p*-GaN of the UV-C LED on sapphire. The results show that the transmittance decreases as the wavelength is shortened, and the light of 254 nm wavelength is almost 0%. Initially, the transmittance for the 450 nm thick *p*-GaN is 0%, but as the *p*-GaN is gradually removed, the transmittance increases. Specifically, for the light of 278 nm, the transmittance increases significantly when the remaining *p*-GaN thickness is less than 60 nm. The transmittance is expressed as follows

$$T = Ae^{-\alpha x}, \quad (1)$$

where A is a coefficient, α is an absorption coefficient (cm^{-1}), and x is the thickness of the material. Fitting the experimental data leads to the following equation $T = 18.7e^{-(1.25\times10^5)x}$, where x is the thickness of *p*-GaN. According to this equation, we obtain an absorption coefficient of $1.25 \times 10^5\ cm^{-1}$ at 278 nm, which is consistent with the absorption coefficients of approximately $1.5 \times 10^5\ cm^{-1}$ reported by Muth et al.[31]

Figures 5(a)–5(c) show the charge-coupled device (CCD) emission image [Fig. 5(a)], the line-profile of the emission distribution [Fig. 5(b)], and the three-dimensional emission distribution [Fig. 5(c)] of the vertical LED without an internal reflector at an injection current of 200 mA. The CCD emission image, the line-profile of the emission distribution, and the three-dimensional emission distribution of the vertical LED with an internal reflector are shown in Figs. 5(d)–5(f), respectively.

As shown in Fig. 5(a), locations on the edge of the chip away from the hole, such as the right top area of chip, exhibit lower intensity. This indicates that highly resistive UV-C LEDs are affected by the current crowding. In Fig. 5(b), the blue line (A-A′) is the line-profile of the emission in the horizontal direction passing through the mesa hole. The inside of the hole exhibits the lowest intensity because it is not the emission area. While the edge of the mesa exhibits the highest intensity. The red line (B-B′), which is the line-profile of the active area, exhibits similar intensity except for the chip edge, similar to the midpoint between the holes of A-A′. Figure 5(c) shows a three-dimensional distribution of emission intensity. As shown in Figs. 5(b) and 5(c), only the area around the hole has high emission intensity.

In Fig. 5(d), the area with an internal reflector shows the brightest image. In Figs. 5(d) and 5(e), the blue line (C-C′) is the line-profile of emission in the horizontal direction passing through the mesa hole. As was the case in Fig. 5(b), the emission intensity is high at the mesa edge. However, the emission intensity at the internal reflector, which is the midpoint between the holes, is higher than that at the mesa edge. Similarly, in the red line (D-D′), the line-profile of emission at the active area with no holes shows the highest emission intensity at the internal reflector, and the areas with the internal reflector show nearly the same emission intensity. This indicates that the hexagonal internal reflector surrounding the hole increases the light reflection. Figure 5(f) shows the three-dimensional distribution of emission intensity for the vertical LED with an internal reflector. The emission intensity is the highest at an internal reflector, so higher emission is observed at an internal reflector compared to the vertical LED without an internal reflector shown in Fig. 5(c).

In conclusion, we have demonstrated a UV-C chip design that is composed of a Ga-face *n*-contact type vertical LED with an internal reflector. The internal reflector in the vertical LED is designed in the form of a hexagon surrounding a *n*-electrode, and is fabricated using a SiO_2/Al reflector. The LOP of the vertical LED with an internal reflector is 1.27 times higher than that of the vertical LED without an internal reflector. The increased light emission for the vertical LED with an internal reflector is attributable to the effective light reflection on the internal reflector as well as improved local reflectivity.

Acknowledgments This research was supported by LG Innotek Co, Ltd. and the Nano Material Technology Development Program through the National Research Foundation of Korea (NRF-2016M3A7B4910429)

1) H. Hirayama, J. Appl. Phys. **97**, 091101 (2005).
2) K. B. Nam, J. Li, M. L. Nakarmi, J. Y. Lin, and H. X. Jiang, Appl. Phys. Lett. **81**, 1038 (2004).
3) A. Khan, K. Balakrishnan, and T. Katona, Nat. Photonics **2**, 77 (2008).
4) M. Kneissl, T. Kolbe, C. Chua, V. Kueller, N. Lobo, J. Stellmach, A. Knauer, H. Rodriguez, S. Einfeldt, and Z. Yang, Semicond. Sci. Technol. **26**, 014036 (2011).
5) I. V. Rozhansky and D. A. Zakheim, Phys. Status Solidi A **204**, 227 (2007).
6) Y. Gao, Q. Chen, S. Zhang, H. Long, J. Dai, H. Sun, and C. Chen, IEEE Trans. Electron Devices **66**, 2992 (2019).
7) R. Liang, J. Dai, L. Xu, J. He, S. Wang, Y. Peng, H. Wang, L. Ye, and C. Chen, IEEE Trans. Electron Devices **65**, 2498 (2018).
8) Y. K. Ooi and J. Zhang, IEEE Photonics J. **10**, 8200913 (2018).
9) M. Shatalov et al., Semicond. Sci. Technol. **29**, 084007 (2014).
10) K. B. Nam, J. Li, M. L. Nakarmi, Y. J. Lin, and H. X. Jiang, Appl. Phys. Lett. **84**, 5264 (2004).
11) H. Y. Ryu, I. G. Choi, H. S. Choi, and J. I. Shim, Appl. Phys. Express **6**, 062101 (2013).
12) T. Kolbe, A. Knauer, C. Chua, Z. Yang, S. Einfeldt, P. Vogt, N. M. Johnson, M. Weyers, and M. Kneissl, Appl. Phys. Lett. **97**, 171105 (2010).
13) Y. Muramoto, M. Kimura, and S. Nouda, Semicond. Sci. Technol. **29**, 084007 (2014).
14) Y. Zhang, S. Krishnamoorthy, F. Akyol, S. Bajaj, A. A. Allerman, M. W. Moseley, A. M. Armstrong, and S. Rajan, Appl. Phys. Lett. **110**, 201102 (2017).
15) H. Hirayama, N. Maeda, S. Fujikawa, S. Toyoda, and N. Kamata, Jpn. J. Appl. Phys. **53**, 100209 (2014).
16) Q. Chen, H. Zhang, J. Dai, S. Zhang, S. Wang, J. He, R. Liang, Z. H. Zhang, and C. Chen, IEEE Photonics J. **10**, 610087 (2018).
17) J. W. Lee, D. Y. Kim, J. H. Park, E. F. Schubert, J. Kim, J. Lee, Y. Kim, Y. Park, and J. K. Kim, Sci. Rep. **6**, 22537 (2016).
18) T. Takano, T. Mino, J. Sakai, N. Noguchi, K. Tsubaki, and H. Hirayama, Appl. Phys. Express **10**, 031002 (2017).
19) H. K. Kim, T. Y. Seong, I. Adesida, C. W. Tang, and K. M. Lau, Appl. Phys. Lett. **84**, 1710 (2004).
20) V. Adivarahan, S. Wu, J. P. Zhang, A. Chitnis, M. Shatalov, V. Mandavilli, R. Gaska, and M. A. Khan, Appl. Phys. Lett. **84**, 4762 (2004).
21) L. Li, T. Tsutsumi, Y. Miyachi, M. Miyoshi, and T. Egawa, Semicond. Sci. Technol. **30**, 125012 (2015).
22) B. K. SaifAddin, A. Almogbel, C. J. Zollner, H. Foronda, A. Alyamani, A. Albadri, M. Iza, S. Nakamura, S. P. DenBaars, and J. S. Speck, Semicond. Sci. Technol. **34**, 035007 (2019).
23) T. Inazu et al., Jpn. J. Appl. Phys. **50**, 122101 (2011).
24) C. H. Kuo, H. C. Feng, C. W. Kuo, C. M. Chen, L. W. Wu, and G. C. Chi, Appl. Phys. Lett. **90**, 142115 (2007).
25) H. K. Cho, O. Krüger, A. Külberg, J. Rass, U. Zeimer, T. Kolbe, A. Knauer, S. Einfeldt, M. Weyers, and M. Kneissl, Semicond. Sci. Technol. **32**, 12LT01 (2017).
26) K. Kawasaki, C. Koike, Y. Aoyagi, and M. Takeuchi, Appl. Phys. Lett. **89**, 261114 (2006).
27) W. S. Wong, T. Sands, N. W. Cheung, M. Kneissl, D. P. Bour, P. Mei, L. T. Romano, and N. M. Johnson, Appl. Phys. Lett. **75**, 1360 (1999).
28) W. H. Chen et al., Appl. Phys. Lett. **91**, 121114 (2007).
29) G. D. Hao, M. Taniguchi, N. Tamari, and S. I. Inoue, J. Phys. D: Appl. Phys. **49**, 235101 (2016).
30) S. Zhang, F. Wu, S. Wang, H. Zhang, Y. Zhang, L. Xu, J. Dai, and C. Chen, IEEE Trans. Electron Devices **66**, 2997 (2019).
31) J. F. Muth, J. H. Lee, I. K. Shmagin, R. M. Kolbas, H. C. Casey, B. P. Keller Jr, U. K. Mishra, and S. P. DenBaars, Appl. Phys. Lett. **71**, 2572 (1997).